Resolving mantle and magmatic processes in basalts from the Cameroon volcanic line using the Re–Os isotope system

Abdelmouhcine Gannoun, Kevin W Burton, Dan Barfod, Pierre Schiano, Ivan Vlastélic, Alex Halliday

Resolving mantle and magmatic processes in basalts from the Cameroon volcanic line using the Re–Os isotope system

A. Gannoun [a,b,*], K.W. Burton [c], D.N. Barfod [d], P. Schiano [a], I. Vlastélic [a], A.N. Halliday [e]

[a] *Laboratoire Magmas et Volcans, Université Blaise Pascal, CNRS-IRD, BP 10448, 63000 Clermont Ferrand, France*
[b] *Department of Earth Sciences, The Open University, Walton Hall, Milton Keynes MK7 6AA, United Kingdom*
[c] *Department of Earth Sciences, Durham University, Science Labs, Durham DH1 3LE, United Kingdom*
[d] *Argon Isotope Facility, NERC/SUERC, East Kilbride G75 1QF, United Kingdom*
[e] *Department of Earth Sciences, University of Oxford, South Parks Road, Oxford OX1 3AN, United Kingdom*

This study presents major-, trace element and Re–Os isotope and elemental data for young alkaline basalts (<10 Ma) from oceanic (Annobon, S. Tomé, Principe), continental (Manengouba) and continent–oceanic bound-ary (COB, Mt. Cameroon) sectors of the Cameroon volcanic line (CVL). The CVL is a chain of Tertiary to recent, transitional to strongly alkaline intraplate volcanoes extending from the south Atlantic island of Annobon to the continental interior of West Africa (Biu Plateau). The basalts from the oceanic sector display a range of initial $^{187}Os/^{188}Os$ ratios between 0.128 and 0.190 and those from the COB and continental sector range between 0.142 and 0.560. The samples with high $^{206}Pb/^{204}Pb$ (e.g. ratios >20) possess $^{187}Os/^{188}Os$ isotope compositions between 0.14 and 0.18 (e.g., basalts from Mt Cameroon and Sao Tomé) which reflect the chemical characteristics that are more likely to be primary features of CVL, and are close to the value of 0.153 attributed to the HIMU end-member (Tubuai–Mangaia). However, most of the lavas from the continental sector show highly radiogenic initial $^{187}Os/^{188}Os$ ratios (0.36 to 0.56) that are outside the range previously observed for ocean island basalts, with shifts to radiogenic Os isotope com-positions accompanied by less radiogenic $^{206}Pb/^{204}Pb$ and increasing SiO_2 contents. The increase in $^{187}Os/^{188}Os$ is also associated with the decrease of Os, Ni, MgO and phenocryst abundances. These data can be explained by fractional crystallisation and assimilation of continental crust by the ascending magma. The systematic shift to unradiogenic lead isotope compositions from the COB into the oceanic sector is positively correlated with variations in $^{187}Os/^{188}Os$ isotope composition (from 0.140 to 0.128). At first sight this covariation might be attributed to the mixing of HIMU material with the ambient upper mantle (DMM). However, there is a clear covariation of the Os isotope and elemental composition, best explained with contamination of the oceanic basalts by the physical entrainment of xenoliths and xenocrysts of mantle origin. Overall, these results indicate that Os in CVL basalts is highly susceptible to contamination from both oceanic and continental lithospheres, under these circumstances covariations with other isotopes and elements must be interpreted with caution.

1. Introduction

A fundamental objective of mantle geochemistry is to understand the scale and nature of the chemical heterogeneity of the mantle that is sampled by basaltic volcanism. Isotopic variations in oceanic basalts are generally ascribed to mixing and/or ageing relationships between different, variably 'depleted' and 'enriched', components in the Earth's mantle (Hart, 1988; Hofmann, 1997; White, 1985; Zindler and Hart, 1986). Of these, DMM ('depleted' mid-ocean ridge basalt (MORB) mantle) is generally considered to represent the Earth's upper mantle depleted in incompatible elements during the formation of the continental crust. Whereas, the various enriched components (HIMU, high $^{238}U/^{204}Pb$ mantle; EM1, 'enriched' mantle 1; and EM2, 'enriched' mantle 2) are thought to reflect recycling processes or intra-mantle differentiation. For example, the chemical characteristics of the HIMU source (radiogenic Pb and unradiogenic Sr) are generally attributed to ancient basaltic oceanic crust stored in the mantle for considerable periods of time (i.e. 1 Gyr or more; Chase, 1981; Chauvel et al., 1992; Hofmann and White, 1982).

The Re–Os isotope system is sensitive to the processes of mantle melting, and the generation and recycling of oceanic crust. This is because Os behaves as a strongly compatible element during melting and is preferentially retained in the mantle, whereas Re is moderately

* Corresponding author at: Laboratoire Magmas et Volcans, Université Blaise Pascal, CNRS-IRD, BP 10448, 63000 Clermont Ferrand, France. Tel.: +33 4 73346706; fax: +44 4 73346739.
E-mail address: M.Gannoun@opgc.univ-bpclermont.fr (A. Gannoun).

incompatible and enters the melt (e.g. Allègre and Luck, 1980; Hauri and Hart, 1993; Shirey and Walker, 1998). Consequently, oceanic (and continental) crust acquires very high Re/Os ratios, and develops radiogenic Os isotope compositions over relatively short periods of time (Dale et al., 2007; Gannoun et al., 2004, 2007; Hauri and Hart, 1993; Shirey and Walker, 1998). Pioneering studies of the Re–Os systematics in ocean island basalts (OIB) provided strong support for the role of oceanic crust in the HIMU mantle, and have demonstrated the utility of this system as a tracer of mantle sources (Class et al., 2009; Hauri and Hart, 1993; Marcantonio et al., 1995; Reisberg et al., 1993; Schiano et al., 2001; Skovgaard et al., 2001).

However, the Re–Os isotope system is also highly susceptible to a number of magmatic processes that may act to obscure the primary mantle signal. For example, it has been shown that some magmatic phases (e.g. olivine, clinopyroxene, …) possess extremely high Re/Os (parent/daughter) ratios (Burton et al., 2002; Gannoun et al., 2004). Consequently, within sample Os isotope heterogeneity in the constituant phases can develop in very short periods of time (several 100 kyr or less). This may well explain why aphyric basalts (i.e. those without phenocryst) tend to yield reproducible Os isotope data and display good correlations between Os and Sr–Nd–Pb, whereas phyric basalts (i.e. those with phenocrysts) are generally less well correlated with other isotope systems (e.g. Schiano et al., 2001). Assimilation of oceanic or continental crust, with a radiogenic Os isotope composition, with concomitant fractional crystallisation (producing magmas with decreasing Os concentrations) seems likely to also have an effect on magma compositions. Such process has been documented in several studies (e.g. Alves et al., 2002; Gleißner et al., 2012; Hart et al., 1997; Lassiter and Luhr, 2001). Finally, recent studies have shown that mantle minerals, not only sulphide but also silicates, generally possess Os concentrations some ~10^2 greater than magmatic phases (e.g. Burton et al., 1999, 2000; Gannoun et al., 2004) although some doubts remain if Os in silicate was indeed located in the lattice. Many OIB contain xenoliths and xenocrysts of mantle origin, and their assimilation, or physical entrainment within samples, could have a significant affect on the Os isotope chemistry of the basalt host.

The Cameroon Line is an alkaline volcanic province that straddles both oceanic and continental lithospheres. Combined Pb, Sr, Nd and Hf isotope studies have shown that in the vicinity of the continent–ocean boundary the lavas have many isotopic characteristics typical of a HIMU source, although the Pb is not as radiogenic as the classic oceanic HIMU localities. This study presents new Os isotope data for a suite of basalts and xenoliths from the Cameroon Line, for which major and trace elements and Pb and Nd isotope data have already been obtained. These results show that Cameroon volcanic line lavas possess Os isotope compositions with the typical HIMU signature. However, lavas from the continental sector show clear evidence of assimilation of material with radiogenic Os during fractional crystallisation, whereas, samples from the oceanic sector show Os isotope and elemental trends that strongly suggest that contamination by lithospheric mantle material has occurred.

2. Geological background and sample selection

The CVL is an alkaline volcanic province extending some 1600 km from the African continental interior into the Gulf of Guinea (Fig. 1). The petrology, geochemistry and geochronology of the Cameroon Line basalts have been extensively documented elsewhere (Aka et al., 2004; Fitton, 1987; Fitton and Dunlop, 1985; Halliday et al., 1988; 1990; Lee et al., 1994; Rankenburg et al., 2005; Yokoyama et al., 2007), and as such only the salient features are discussed here. Magmatic activity in the Cameroon Line extends over at least the past 65 Myr to the present but shows no systematic migration with time as might be expected for plume track migration (typified by the Hawaiian hot spot). Most of the volcanic centres along the entire length of the chain have recently been active. There are at least 17 plutonic complexes in

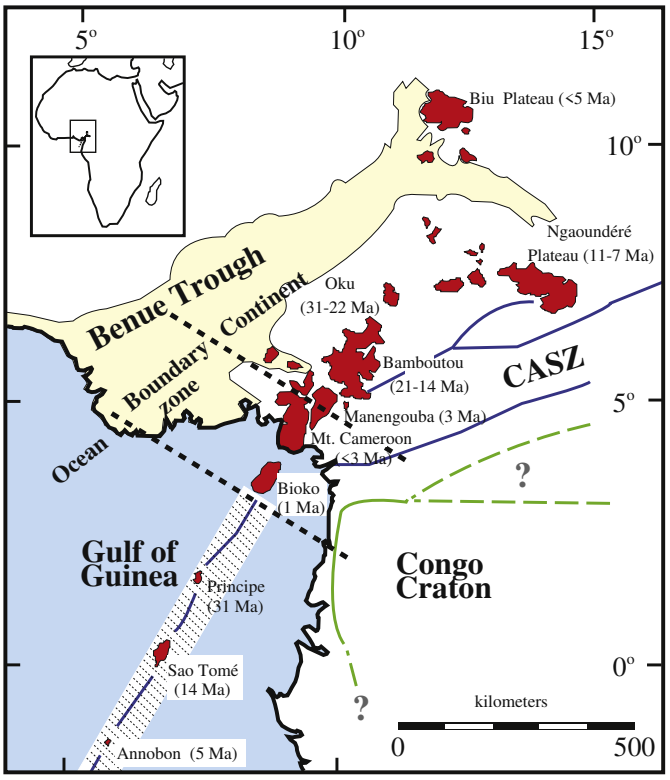

Fig. 1. Map of the main geological features of the area of the Cameroon Line and the Gulf of Guinea showing the distribution of the main Cenozoic volcanic centres (in red), the definition of the continent/ocean boundary region and the eruption ages of the major volcanic centres (adapted from Fitton and Dunlop, 1985). Ages are compiled from Fitton and Dunlop (1985), Halliday et al. (1990), and Lee et al. (1994). The thick blue lines trending east-northeast mark the Central African Shear Zone (CASZ). The stippled white box offshore is the inferred location of the Cameroon Fracture Zone (Sibuet and Mascle, 1978). The location of the Congo Craton is shown by the green line, however the exact location for the boundary to the northeast and west is not well known and possible locations of the boundary are shown with dashed green lines (after Schlüter, 2006; Reusch et al., 2010). The basement between the Congo Craton and the Benue Trough is comprised of the Oubanguides mobile belt.

the continental sector, ranging in age from 65 Ma to 30 Ma. Geochemical data indicate that these complexes are primarily of mantle origin but are contaminated by crustal components (Jacquemin et al., 1982; Parsons et al., 1986; Rankenburg et al., 2005). In addition there are 12 major volcanic centres extending into the oceanic sector ranging in age from 35 Ma to the present. The CVL can be divided into three zones: the oceanic sector (Annobon, Principe and São Tomé), the continent/ocean boundary (COB: Bioko and Mt. Cameroon) and the continental sector (Manengouba, Bamboutou, Oku, Ngaoundéré Plateau and Biu Plateau). The only currently active volcano is Mt. Cameroon (COB) which erupted last in 2000 (Suh et al., 2003). The volcanic centres in the CVL erupt mostly alkaline basalts, along with minor tholeiitic basalts and evolved rocks (phonolites and trachytes; Fitton and Dunlop, 1985).

Major and trace element patterns of the mafic rocks (≥4.0 wt.% MgO) are similar in both continental and oceanic sectors, suggesting that the lavas have not been significantly modified during ascent through the lithosphere. When compared with other representative mantle end-members the CVL basalts are close to those of a HIMU-type (Fig. 2), characterised by their enrichment in incompatible trace elements. As HIMU basalts, the CVL lavas share the same negative anomalies of K, and Pb which are complementary to the corresponding positive anomalies in average continental crust. Similarly, they show a decrease in the normalised abundances of the most incompatible elements (Rb, Ba), which indicates a depleted 'heritage' for HIMU OIB

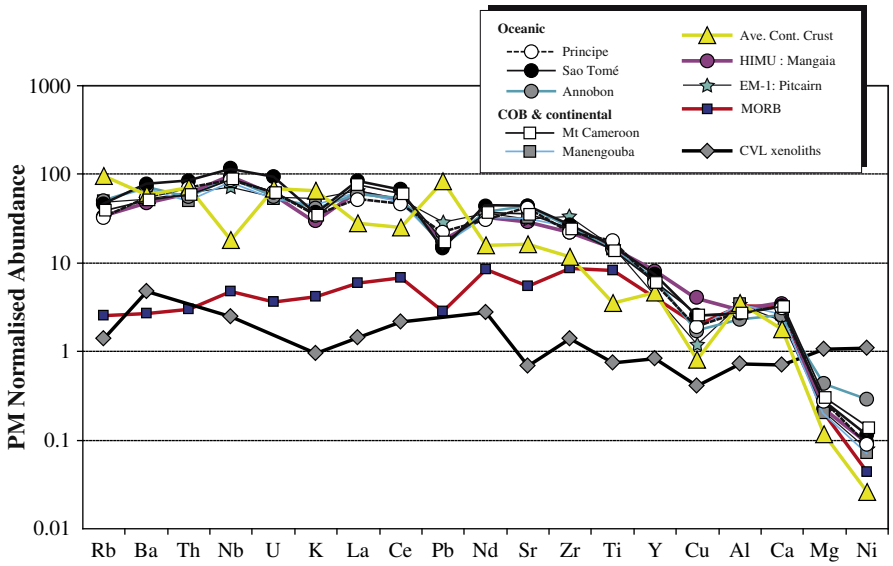

Fig. 2. Primitive-mantle normalised trace and major element abundance diagrams ("spidergrams") for CVL basalts. Only the average for each volcanic centre is plotted. No apparent differences between continental and oceanic sectors. Representative samples of HIMU (Mangaia, Austral islands; Woodhead (1996)), EM-1 (Pitcairn; Eisele et al. (2002)), average continental crust (Rudnick and Fountain, 1995), and average normal MORB (Atlantic and Pacific, A. Gannoun unpublished data) are also plotted. As HIMU basalts, CVL lavas are sharing the same negative anomalies of Rb, K, and Pb which are complementary to the corresponding positive anomalies in average continental crust. Similarly, the positive spike of Nb in CVL basalts is balanced by negative one in continental crust. All abundances are normalised to primitive mantle values of McDonough and Sun (1995).

(Hofmann, 1997), and the enrichment of Nb in CVL basalts is balanced by a depletion of this element in the continental crust.

Combined isotopic studies reveal temporal and spatial patterns in the mafic rocks of the CVL. At the continent–ocean boundary (COB) young (<10 Ma) lavas possess relatively radiogenic Pb ($^{206}Pb/^{204}Pb \sim 20.5$) and unradiogenic Nd ($\varepsilon_{Nd} \sim +3$) compositions, but with distance away from the COB have less radiogenic Pb ($^{206}Pb/^{204}Pb \sim 19.0$) and more radiogenic Nd ($\varepsilon_{Nd} \sim +6$). Lavas from Mount Cameroon and the ocean islands show systematic shifts to more radiogenic Pb and Sr and less radiogenic Nd with decreasing age (Halliday et al., 1990; Lee et al., 1994). The earliest lavas from Principe (31 Ma) and Sao Tomé (13 Ma) have very similar Pb, Sr and Nd isotope compositions to those of Annobon (<5 Ma) (Lee et al., 1994). These observations are consistent with a common source for all islands with the later lavas being affected by interaction with other mantle components. Although the Cameroon Line does not possess Pb as radiogenic as that of the classic HIMU localities, such as Tubuai or Mangaia (e.g. Chauvel et al., 1992; Woodhead, 1996), it does possess major, trace-element and isotope compositions that are indistinguishable from those of other HIMU OIB (Halliday et al., 1988, 1990; Lee et al., 1994) However, the nature of the Cameroon Line HIMU remains a subject of debate. Some have argued that this HIMU signature reflects recent enrichment of the oceanic upper mantle that occurred at the time of formation of the local oceanic lithosphere and has been preserved in the uppermost mantle for 125 Myr (e.g. Halliday et al., 1990). Furthermore, on the basis of the low $^{207}Pb/^{204}Pb$ (for a given $^{206}Pb/^{204}Pb$), the CVL has been interpreted in terms of remelting of an enriched fossil plume head located beneath the COB (Halliday et al., 1990). Others have argued that the common source for all islands in CVL from which melting is initiated could be ambient upper mantle with unradiogenic Pb entrained within a plume head during ascent. The progression to radiogenic Pb reflects the increasing importance of an active plume stem composed of relatively uncontaminated HIMU mantle (Lee et al., 1994).

In this study, 21 mafic volcanic samples have been analysed, that range in composition from alkali basalt, to basanite and picro-basalt (Barfod, 1999). Sample localities are given in Table 1. Thirteen samples are from islands in the oceanic sector including Annobon, Sao Tomé and Principe. Six samples from Mt. Cameroon (COB) and two samples from Manengouba (continental sector) were also analysed. Olivine and clinopyroxene are the major phenocrysts in this sample suite, with minor plagioclase. In order to better understand distribution and behaviour of Re–Os isotopes amongst magmatic phases, and the potential impact of xenocrysts on the lava chemistry, Os isotopes have also been measured in olivines and clinopyroxene separated from two of the oceanic lavas.

In addition, in order to characterise the Os signature of the sub-lithospheric mantle beneath the CVL, six basalt-hosted ultramafic xenoliths (Lee et al., 1996) have also been analysed in this study. All of these were collected from the major continental volcanic centres of the CVL (Table 1). The petrology and geochemistry of the ultramafic xenoliths have been extensively described elsewhere (Barfod, 1999; Lee et al., 1996; Rehkämper et al., 1997). All the xenoliths are thought to be depleted residues after the extraction of basaltic melts from an upper mantle similar to the present day Atlantic MORB mantle source (Lee et al., 1996), but some preserve evidence of interaction with enriched partial melts before entrainment. Five of the six xenoliths are spinel lherzolite which are fertile with 10 to 15% clinopyroxene. The only harzburgite analysed N12, with only ~5% clinopyroxene is markedly enriched in LREE $[(La/Yb)_N = 4.1]$ attesting to the metasomatic enrichment processes that are thought to have affected the Cameroon Line mantle lithosphere during the Mesozoic (Lee et al., 1996).

3. Analytical techniques

Basalt samples were crushed in agate mortar and between 0.5 and 1 g of powdered rock were used for Re–Os isotope analysis. The basalt samples were spiked with a mixed ^{185}Re and ^{190}Os spike. The dissolution was achieved using HF–HBr in a Savillex Teflon bomb heated at 150 °C for at least 2 days. This step was followed by oxidation of Os to OsO_4 in a nitric acid solution containing chromium trioxide to ensure spike/sample osmium isotopic homogenisation, Os was then extracted in liquid bromine and purified by micro-distillation (Birck et al., 1997). The remaining aqueous solution containing Re was reduced with ethanol and Re was extracted and purified by liquid/liquid extraction with iso-amylic alcohol and 2 N HNO_3. Rhenium and osmium were analysed as negative ions, using the ion counting electron multiplier on a Thermo-Electron TRITON® thermal ionisation mass spectrometer at the Open University. Whole-rock total procedural blanks for Os during

Table 1
Re–Os abundance and Os isotope data for basalts and ultramafic xenoliths from Cameroon volcanic line.

Sample	Location	Lithology	Coordinates	Age[a] (Ma)	SiO_2[b] (wt.%)	MgO[b] (wt.%)	Ni[b] (ppm)	Phenocryst (vol. %)[b]		$^{187}Os/^{188}Os$[c]	$^{187}Os/^{188}Os_i$	$^{187}Re/^{188}Os$[d]	Re (ppt)	Os (ppt)	Blank (%)	
								Olivine	Clinopyroxene						(Os)	(Re)
Oceanic basalts																
A22	Annobon	Basanite	1° 26.0′ S; 5°38.0′ E	4.60 ± 0.07	43.90	10.32	214	10	20	0.1357 ± 0.0015	0.1288 ± 0.0016	90.4	410	22.25	0.3	1.0
A3	Annobon	Basanite	1° 25.2′ S; 5°36.8′ E	<0.1	42.02	16.90	623	10	2	0.1280 ± 0.0003	0.1280 ± 0.0003	27.7	407	70.72	0.1	1.1
Dupl.[e]										0.1283 ± 0.0002	0.1283 ± 0.0002	29.8	421	68.94	0.2	0.8
A5	Annobon	Basanite	1° 25.5′ S; 5°36.8′ E	4.93 ± 0.08	43.70	20.84	717	30	3	0.1352 ± 0.0004	0.1308 ± 0.0005	52.7	357	32.69	0.2	1.2
Dupl.[e]										0.1366 ± 0.0003	0.1321 ± 0.0004	54.8	350	31.19	0.5	1.0
A7	Annobon	Basanite	1° 25.5′ S; 5°37.2′ E	<0.2	42.11	15.16	546	15	0	0.1315 ± 0.0005	0.1314 ± 0.0005	10.8	205	91.35	0.1	2.2
Dupl.[e]										0.1321 ± 0.0004	0.1321 ± 0.0004	11.0	212	93.80	0.2	1.7
ST106	São Tomé	Basanite	0° 20.9′ N; 6°39.5′ E	3.00 ± 0.07	44.08	13.19	390	20	1	0.1482 ± 0.0011	0.1441 ± 0.0012	82.7	237	13.86	0.5	1.9
ST201	São Tomé	Basanite	0° 20.9′ N; 6°39.5′ E	<0.2	44.17	10.24	224	10	5	0.1468 ± 0.0013	0.1459 ± 0.0013	279	232	4.012	1.6	1.8
ST218	São Tomé	Basanite	0° 22.0′ N; 6°38.5′ E	0.77 ± 0.05	41.10	10.22	205	5	5	0.1433 ± 0.0011	0.1395 ± 0.0013	300	578	9.303	0.8	0.9
Dupl.[e]										0.1450 ± 0.0008	0.1412 ± 0.0010	303	610	9.833	1.5	0.6
ST223	São Tomé	Picro-basalt	0° 00.0′ N; 6°00.0′ E	8.7 ± 0.4	43.38	12.79	220	5	30	0.1474 ± 0.0005	0.1443 ± 0.0006	21.0	465	107.0	0.1	1.0
Dupl.[e]										0.1486 ± 0.0004	0.1455 ± 0.0005	21.4	484	110.23	0.2	0.8
ST227	São Tomé	Basanite	0° 00.0′ N; 6°00.0′ E	<0.2	42.67	10.69	223	10	0	0.1884 ± 0.0009	0.1876 ± 0.0010	248	318	6.223	1.0	1.4
Dupl.[e]										0.1901 ± 0.0006	0.1893 ± 0.0006	232	331	7.002	2.1	1.0
ST228	São Tomé	Basanite		<0.2	42.45	10.61	212	10	1	0.1718 ± 0.0013	0.1714 ± 0.0013	118	159	6.553	0.8	2.4
ST231	São Tomé	Tephrite	0° 00.0′ N; 6°00.0′ E	0.90 ± 0.05	45.58	5.82	84	1	2	0.1885 ± 0.0027	0.1821 ± 0.0031	423	408	4.681	1.4	1.1
P102	Príncipe	Basanite	1° 38.1′ N; 7°25.4′ E	5.92 ± 0.09	43.69	8.59	136	7	30	0.1380 ± 0.0021	0.1338 ± 0.0022	42.3	143	16.38	0.4	2.7
P119	Príncipe	Picro-basalt	1° 39.7′ N; 7°26.7′ E	20.4 ± 0.3	41.60	11.90	216	15	25	0.2056 ± 0.0015	0.1280 ± 0.0018	226	599	12.87	0.5	0.7
COB and continental basalts																
C237	Mt. Cameroon	Basalt	4° 00.0′ N; 9°00.0′ E	1.84 ± 0.07	46.88	9.34	191	10	1	0.5338 ± 0.0074	0.5183 ± 0.0080	504	273	2.745	2.4	1.7
C238	Mt. Cameroon	Basalt	4° 00.0′ N; 9°00.0′ E	1.86 ± 0.07	47.01	8.96	361	5	1	0.4715 ± 0.0027	0.4641 ± 0.0029	241	204	4.258	1.4	2.0
Dupl.[e]										0.4826 ± 0.0019	0.4755 ± 0.0022	228	212	4.737	2.9	1.5
C26	Mt. Cameroon	Basanite	4° 00.0′ N; 9°00.0′ E	1922 eruption	42.79	8.85	135	7	15	0.1449 ± 0.0043	0.1449 ± 0.0043	107	403	18.16	0.3	1.0
Dupl.[e]										0.1458 ± 0.0015	0.1458 ± 0.0015	106	411	18.96	0.8	0.8
C30	Mt. Cameroon	Basanite	4° 00.0′ N; 9°00.0′ E	<0.2	44.72	12.81	260	20	20	0.1424 ± 0.0007	0.1422 ± 0.0007	57.6	500	41.96	0.2	0.9
Dupl.[e]										0.1436 ± 0.0005	0.1434 ± 0.0005	58.2	513	43.01	0.4	0.7
C4	Mt. Cameroon	Basalt		<0.2	45.62	9.06	131	5	30	0.1500 ± 0.0005	0.1495 ± 0.0005	132	579	21.19	0.3	0.8
R14	Mt. Cameroon	Picro-basalt	4° 00.0′ N; 9°00.0′ E	<0.2	43.44	20.09	611	30	3	0.1533 ± 0.0003	0.1531 ± 0.0003	42.4	612	69.77	0.1	0.6
C239	Manengouba	Basalt	5° 02.0′ N; 9°49.2′ E	<0.2	45.87	8.34	145	7	5	0.5592 ± 0.0035	0.5565 ± 0.0035	822	1083	6.708	1.1	0.5
Dupl.[e]										0.5563 ± 0.0018	0.5536 ± 0.0018	808	1144	7.278	2.1	0.3
C247	Manengouba	Basalt	5° 02.0′ N; 9°49.2′ E	<0.2	50.64	6.53	125	5	5	0.3706 ± 0.0031	0.3683 ± 0.0031	677	321	2.358	2.8	1.4
Mantle xenoliths																
N12[e]	Biu Plateau	Harzburgite			42.02	46.80	2566			0.1187 ± 0.0002		0.387	202	2540	0.01	3.2
P13[e]	Ngaoundéré	Sp. lherzolite			43.69	39.73	2094			0.1252 ± 0.0008		0.634	226	1734	0.02	3.0
C235A[e]	Mt. Cameroon	Sp. lherzolite			44.06	37.67	1949			0.1270 ± 0.0003		1.687	325	940	0.03	2.1
C235D[e]	Mt. Cameroon	Sp. lherzolite			45.08	37.25	1874			0.1273 ± 0.0002		1.462	389	1296	0.02	1.6
C271I[e]	Oku	Sp. lherzolite			43.97	40.67	2182			0.1212 ± 0.0002		0.496	310	3051	0.01	2.2
C273Q[e]	Oku	Sp. lherzolite			43.94	37.97	2055			0.1248 ± 0.0003				2402	0.01	

[a] Ages represent argon inverse isochrons. ^{40}Ar–^{39}Ar incremental heating analyses were performed at the University of Michigan and the methods are outlined in Conway et al. (1997) and Lee et al. (1994).
[b] Data for basalts are taken from Barfod (1999) and for mantle xenoliths from Lee et al. (1996).
[c] All errors are $2\sigma_m$. $^{187}Os/^{188}Os$ normalised to $^{192}Os/^{188}Os = 3.08271$; given ratios are blank corrected and corrected using measured $^{18}O/^{16}O$ and $^{17}O/^{16}O$ ratios of 0.002047 and 0.00037, respectively.
[d] $^{187}Re/^{188}Os$ ratio determined to a precision of ±1%.
[e] Samples digested with Carius Tube technique.

the course of this study varied between 0.021 and 0.044 pg with an average of Os concentration of 0.033 ± 0.010 (n = 7). The $^{187}Os/^{188}Os$ ratio of the weighted mean is 0.24 ± 0.04. For Re they were between 1.5 and 3.8 pg (n = 7) with a mean value of 2.24 pg. Blank corrections applied to Re and Os concentrations amounted to 0.3–3% and 0.1–3.2% respectively.

Optically pure and inclusion-rich olivine and one clinopyroxene fraction were separated from samples A3 to A7 (Annobon) and were powdered in an agate mortar. The weight of the mineral separates ranged from 15 to 145 mg. The Re–Os chemistry closely follows that used for the whole-rock. Both Re and Os were analysed on Thermo-Electron TRITON® at Blaise Pascal University. The average Os blank was 0.022 pg with $^{187}Os/^{188}Os$ of 0.38 ± 0.05 (n = 4) while the mean value for the Re blank was 1.2 pg (n = 4). Blank corrections applied to Re and Os concentrations for the mineral separates were 1.2–6.7% and 0.1–0.6%, respectively.

It has been shown that low temperature acid digestion (LTAD) may not recover all the Re and Os present in the samples (Meisel et al., 2003), particularly when PGE rich alloy phases are present. Thus, to ensure full recovery of both Re and Os from the studied samples, Carius tube (CT) digestion was used for duplicate measurements of ten basalt samples representative of the entire range analysed for both Os isotope composition and Os abundance obtained by LTAD. CT digestion method was also used for the xenolith samples. Approximately 1 g of each whole rock powder was digested and equilibrated with a mixed ^{185}Re–^{190}Os spike, using inverse aqua regia (2.5 ml of 12 M HCl and 5 ml 16 M HNO3) in a borosilicate CT and placed in an oven at 250 °C for at least 72 h. Osmium was extracted using carbon tetra-chloride (CCl_4), back-extracted using HBr and then microdistilled (Cohen and Waters, 1996). The aqua regia was dried, re-dissolved in 2 M HNO_3, and Re was recovered in iso-amylol and extracted in ultrapure water (Birck et al., 1997). The CT digestion gave, average total procedural blanks of 0.16 pg Os, 3.66 pg Re, and $^{187}Os/^{188}Os$ of 0.39 ± 0.05 (n = 4).

Repeat analyses of 100 pg and 10 pg aliquots of a Johnson Mathey (JM) Os standard gave a mean value of 0.17388 ± 26 (n = 26) and 0.1741 ± 3 (n = 15), respectively, and these were run over the duration of the study. These values are in good agreement with published Faraday cup N-TIMS values (Birck et al., 1997; Nowell et al., 2008).

Duplicate measurements for the ten basalt samples digested using CT are reported in Table 1. The CT digestion method recovers slightly higher Re and Os concentrations, within ±5%, except the three samples possessing the lowest Os abundances measured in this study (i.e. samples ST227, C238 and C239 having Os concentrations between 4 and 7.5 ppt). However, both techniques yield similar $^{187}Os/^{188}Os$ ratios, within ±2%, hence, the two different digestion techniques are in good agreement at least for the basaltic rocks analysed here.

4. Results

4.1. Basalts

Selected major- and trace-element and phenocryst abundances were previously determined (Barfod, 1999) and are reported in the Supplementary Table. Samples vary in composition from Mg-rich basanite to more evolved alkali basalts. Basalt samples from oceanic and continental sectors display the same range of MgO which varies from 5 to 21 wt.%, but most of the samples have >8 wt.% MgO. Samples with high MgO are also rich in olivine phenocrysts and may have been affected by crystal accumulation as confirmed by Ni higher than 400 ppm and Cr higher than 600 ppm.

The Re and Os elemental and isotope data are given in Table 1. The Re concentration of CVL basalts ranges from 143 to 610 ppt, and from 204 to 612 ppt for oceanic and continental sectors, respectively (excluding one Re-rich sample of 1144 ppt from Manengouba which falls in the MORB field (Fig. 3)). The Os concentrations are also similar between both sectors ranging from 4 to 110 ppt and from 2 to 70 ppt,

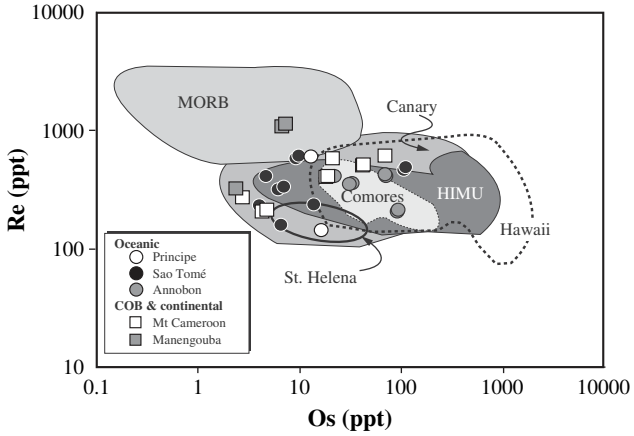

Fig. 3. Rhenium (ppt) against osmium (ppt). CVL basalt field falls within the usual scope of enriched OIB. CVL lavas are less enriched in Re but more enriched in Os than MORB (Gannoun et al., 2007; Schiano et al., 1997). Other literature data are from the following references: Hawaii (Bennett et al., 1996; Hauri et al., 1996; Lassiter and Hauri, 1998); Canary (Marcantonio et al., 1995; Widom et al., 1999); Comores (Class et al., 2009); St. Helena (Reisberg et al., 1993); and HIMU, Cook Australs (Hauri and Hart, 1993; Reisberg et al., 1993; Schiano et al., 2001).

respectively. The CVL basalts lie within the usual range of enriched OIB in terms of Re and Os concentrations (Fig. 3) with most of the samples falling in the HIMU-type Austral–Cook island field (Class et al., 2009; Hauri and Hart, 1993; Reisberg et al., 1993; Schiano et al., 2001). Amongst the basalts studied here only those of the continental sector show a positive co-variation between Os and MgO, Ni and Cr and phenocryst abundance. Samples with high abundances in phenocrysts (olivine + clinopyroxene) are those that are rich in Os, Ni and MgO (Fig. 4), which serves to emphasise the role of olivine accumulation in controlling Os concentrations. The $^{187}Os/^{188}Os$ isotope compositions vary greatly within the CVL basalts ranging from 0.128 to 0.190, and from 0.142 to 0.559, in oceanic and continental sectors, respectively. Age correction only slightly affects the isotopic compositions of a few of the samples, and is less than 5% for all samples except for sample P119, from Principe, which has an age of 20.4 Ma. Therefore, the range of initial isotopic ratios also remains large, between 0.13 and 0.19 and between 0.14 and 0.56 for oceanic and continental sectors, respectively. Many of these isotope compositions are far more radiogenic than those reported for enriched OIB (e.g., Class et al., 2009; Hauri and Hart, 1993; Reisberg et al., 1993; Roy-Barman and Allègre, 1995; Schiano et al., 2001) or those observed for Biu Plateau lavas from the continental sector of the CVL (Rankenburg et al., 2005).

Samples with high $^{206}Pb/^{204}Pb$ (e.g. ratios >20) also have $^{187}Os/^{187}Os$ ratios between 0.14 and 0.18 (e.g., basalts from Mt Cameroon and Sao Tomé) and preserve the characteristics that are more likely to be primary features of CVL lavas. The observed $^{187}Os/^{187}Os$ range for these radiogenic Pb rich samples is close to HIMU-type ($^{187}Os/^{188}Os$ of 0.15–0.16; Hauri and Hart, 1993; Reisberg et al., 1993; Schiano et al., 2001). Basalts from the oceanic sector define a positive co-variation in the Os isotope composition against the reciprocal of the concentration where the three studied islands possess distinctive chemical characteristics (Fig. 5). The least radiogenic samples are those from Annobon (0.128–0.132) which yields a range of Os isotope ratios indistinguishable from those of oceanic mantle (Gannoun et al., 2007; Harvey et al., 2006; Snow and Reisberg, 1995). The homogeneity of $^{187}Os/^{188}Os$ of Annobon lavas is consistent with their relatively uniform Nd and Pb isotope compositions.

4.2. Mineral separates

The Re and Os concentrations and $^{187}Os/^{188}Os$ isotope compositions for olivine and clinopyroxene phenocrysts are given in Table 2. Optically pure olivine from basalts A3 to A7 possesses Os concentrations of

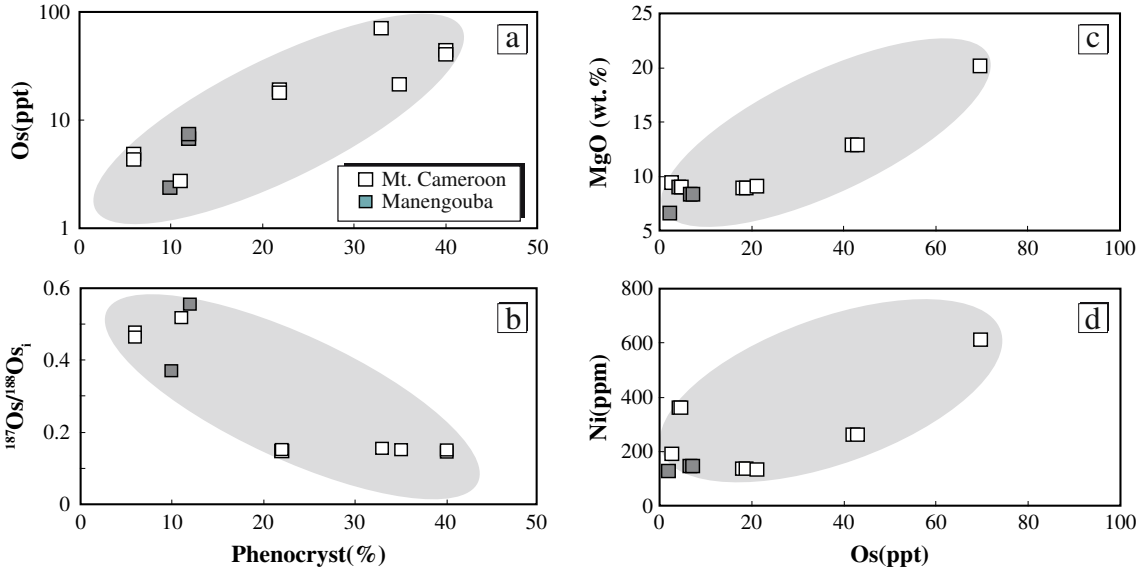

Fig. 4. Evidence of AFC in the CVL basalts from the continental sector. (a) Variation of Os with phenocryst abundances illustrating the effect of the crystallisation of olivine on the Os contents. (b) Os isotope ratios (age corrected) covary also with the phenocryst abundances. The decrease of the latter shows that the most differentiated lavas are the most contaminated by the assimilation of radiogenic continental crust material. Variation of Os with (c) MgO and with (d) Ni contents illustrating the systematic decrease in Os with MgO and Ni as result of fractional crystallisation process.

24–46 ppt, lower than the corresponding whole-rock, while mineral inclusion-rich olivine has higher Os concentrations ranging from 958 to 2654 ppt. The only analysed clinopyroxene from sample A3 has an Os concentration of 325 ppt. Rhenium concentrations for the same silicate phases are 132–338 ppt in pure olivine, 1756–1996 ppt in inclusion-rich olivine and 413 ppt in clinopyroxene. The Re and Os concentrations of the inclusion-rich olivine are consistently higher than their corresponding bulk-rock. Mineral age corrected $^{187}Os/^{188}Os$ isotope compositions range from 0.132 to 0.138 and are consistently higher than the corresponding bulk-rock. In contrast, inclusion-rich olivine has $^{187}Os/^{188}Os$ ratios that are systematically less radiogenic than that of the bulk-rock, even lower than estimates for the present-day primitive upper mantle (i.e. 0.1296 ± 0.0009; Meisel et al., 1996) but within the range of values from mantle peridotites. The $^{187}Re/^{188}Os$ of the mineral phases ranges from 20 to 44 for olivine, 6.2 for clinopyroxene, and from 3.5 to 10.2 for inclusion-rich olivine. The minerals from basalt A7 define a positive correlation in Re–Os isotope evolution diagram with an apparent age of 24 ± 4 Ma. This age is much greater than that obtained by Ar techniques (Table 1), and the covariation between the Os isotope composition and the reciprocal of the concentration suggests that this most likely reflects mixing between the olivine phenocrysts and bulk-rock, rather than having some chronological significance. In this mixing diagram (Fig. 5c) the inclusion-rich olivines possess a composition similar to the mantle xenoliths, suggesting that these crystals are xenocrysts of mantle origin hosting sulphide grains that dominate their chemistry. This interpretation is entirely consistent with petrographic observation that reveals the widespread presence of sulphide-bearing olivine crystals that are not in textural equilibrium with other phases in this rock (Barfod, 1999).

4.3. Xenoliths

The Re–Os isotope and elemental data for the bulk xenolith samples from the Cameroon Line are given in Table 1. The Os concentrations (0.94–3.05 ppb) are similar to other non-cratonic ultramafic xenoliths worldwide (Meisel et al., 2001) but lower than those obtained for orogenic massif peridotites (Reisberg and Lorand, 1995). The Re concentrations range from 0.20 to 0.39 ppb overlapping estimates for fertile mantle, i.e. 0.26 ppb (Morgan, 1986) and the primitive upper mantle (0.35 ppb; Becker et al., 2006). Consequently, most of the samples have supra-chondritic $^{187}Re/^{188}Os$ ratios (i.e. > range of 0.37–0.48, Fischer-Gödde et al., 2010; Walker et al., 2002). However, $^{187}Os/^{188}Os$ ratios range from 0.1187 to 0.1273 and are sub-chondritic to chondritic (chondrite overall ranges between 0.124 and 0.133; Fischer-Gödde et al., 2010; Walker et al., 2002). These observations imply recent addition of Re most probably contemporaneous to the melt enrichment of shallow depleted mantle during the Mesozoic (Lee et al., 1996). The xenoliths display a broad positive correlation between $^{187}Os/^{188}Os$ and $^{187}Re/^{188}Os$ and other elemental proxies of melt depletion (e.g. Al_2O_3, CaO). The Re depletion model ages (that assume complete Re loss at the time of depletion) indicate minimum ages of between 0.2 and 1.4 Ga. The highest age is preserved by the only harzburgite analysed in this study (N12) which possesses the most unradiogenic Os isotope composition (i.e. 0.1187).

5. Discussion

5.1. Fractional crystallisation–continental crust assimilation

The continental alkali basalts of the CVL display unusually radiogenic $^{187}Os/^{188}Os$ compositions even after age correction (i.e. from 0.14 to 0.56). This range of compositions while more radiogenic than those of oceanic basalts and mantle derived xenoliths is comparable to that observed in subduction zone lavas (Alves et al., 2002; Borg et al., 2000; Chesley et al., 2002). It is unclear whether these radiogenic compositions relate to source heterogeneity, or magma interaction with the sub-continental lithospheric mantle or with the continental crust itself. Lavas from the continental sector lie on a mixing trend between a primary composition similar to HIMU lavas and an end member with $^{187}Os/^{188}Os > 0.6$ (Figs. 6; 7). However, Os provides a means for distinguishing the identity of this radiogenic component. The SCLM is ruled out because ultramafic xenoliths sampled from the major continental centres (Mt. Cameroon, Oku, Ngaoundéré and Biu Plateau along an ~600 km long stretch) preserve only unradiogenic isotope compositions from sub-chondritic to chondritic (0.118 to 0.127) and accordingly the derived melts should have similar $^{187}Os/^{188}Os$ ratios. Furthermore the transport kinematics of xenoliths suggest an ascent rate of ~50 cm/s (Morin and Corriveau, 1996) which would result in short residence times (<100 h) for the xenoliths in basaltic magmas (Scarfe and Brearly, 1987). Thus, the extremely radiogenic Os isotope ratios in

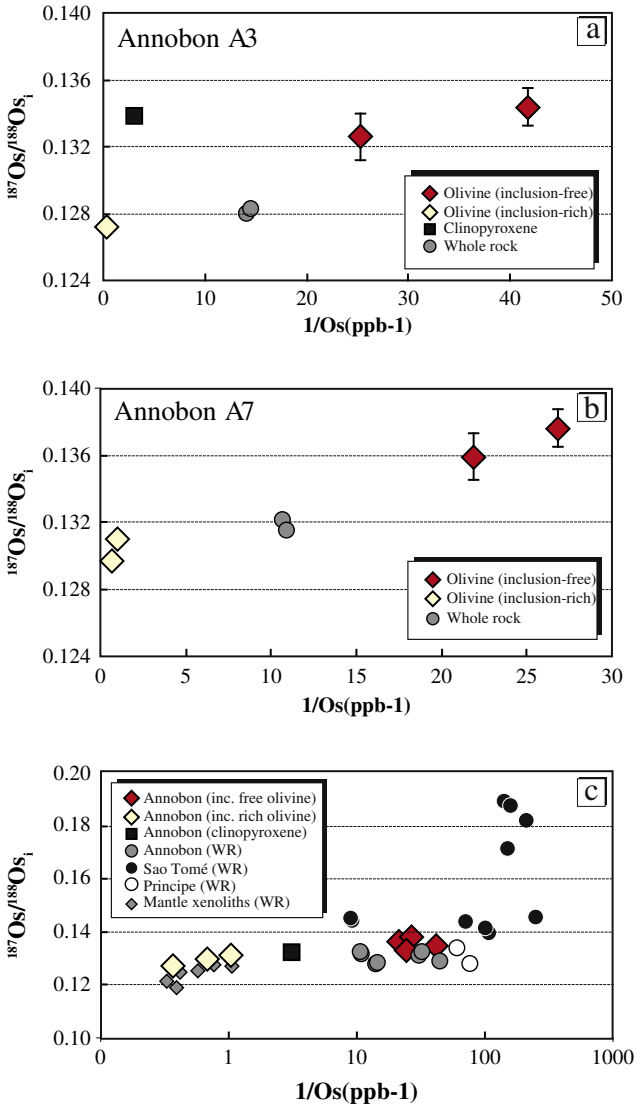

Fig. 5. Initial Os isotope composition in oceanic CVL basalts versus the reciprocal of the Os concentration. (a) and (b) Annobon whole rock lavas and host olivine and cpx phenocrysts. $^{187}Os/^{188}Os$ ratios for clinopyroxene and pure olivine range from 0.132 to 0.138 and remain consistently higher than the corresponding bulk-rock. In contrast, inclusion-rich olivine gives systematically unradiogenic $^{187}Os/^{188}Os$ ratios below that of the bulk-rock and plays a dominant role in Os mass balance at whole rock scale. (c) Inclusion-rich olivine plot close to the mantle xenoliths indicating their xenocrystic origin.

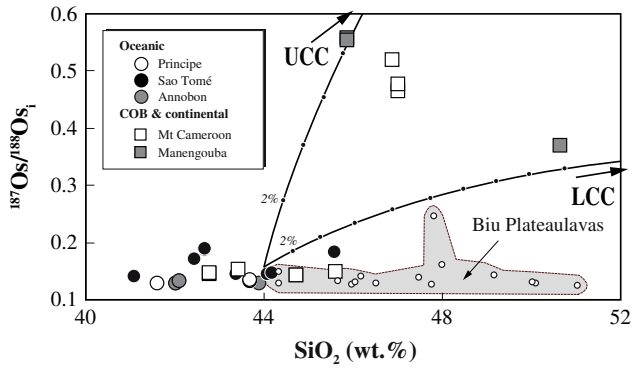

Fig. 6. Variation of initial $^{187}Os/^{188}Os$ ratio versus SiO_2 content of CVL basalts. The most radiogenic samples from the continental sector of the CVL are those with the highest SiO_2 contents. The field of Biu Plateau lavas is added for comparison (Rankenburg et al., 2005). Modelling parameters are as follows: for starting melt, SiO_2 = 44 wt.%, [Os] = 10 ppt, $^{187}Os/^{188}Os$ = 0.156; for upper continental crust (UCC), SiO_2 = 66 wt.%, [Os] = 50 ppt, $^{187}Os/^{188}Os$ = 1.4; and for lower continental crust (LCC), SiO_2 = 59 wt.%, [Os] = 30 ppt, $^{187}Os/^{188}Os$ = 0.8. Increments in the curves are 2%.

continental CVL suggest that the magmas have not experienced significant interaction with SCLM.

The continental CVL lavas with the highest $^{206}Pb/^{204}Pb$ (>20.1) scatter around $^{187}Os/^{188}Os$ values that are thought typical of the HIMU component (0.153) while the samples with $^{206}Pb/^{204}Pb$ < 19.94 show the most elevated $^{187}Os/^{188}Os$ found in this study. The latter samples are also characterised by high SiO_2, low MgO, Ni, and Os and phenocryst abundance (Figs. 4, 6–7). Such trends are most likely to be accounted for by contamination from the continental crust. The decrease in concentration of these compatible elements accompanying differentiation of the lavas is associated with a shift of the $^{187}Os/^{188}Os$ isotope ratios to radiogenic compositions. The differentiated lavas with low Os abundances are more vulnerable to contamination. Therefore, the covariation between the abundances of compatible elements (e.g. Os, Ni and Mg) and the percentage of phenocrysts suggests that contamination might occur through a shallow level coupled assimilation–fractional crystallisation process (AFC), in which fractional crystallisation releases the latent heat that is needed to melt wall-rocks surrounding the magma (e.g. DePaolo, 1981).

Previous studies reported evidence for contamination of some evolved phonolites and trachytes of the continental sector by continental material, based upon radiogenic $^{87}Sr/^{86}Sr$ and unradiogenic $^{143}Nd/^{144}Nd$ isotope compositions (Marzoli et al., 1999) and radiogenic $^{187}Os/^{188}Os$ (Rankenburg et al., 2005). In general, the continental crust possesses radiogenic Os isotope compositions, both the lower and

Table 2
Re–Os isotope data for mineral separates from A3 to A7 basalts of Annobon.

	$^{187}Os/^{188}Os$	$^{187}Os/^{188}Os$[a]	Re (ppt)	Os (ppt)	$^{187}Re/^{188}Os$	Blank Os (%)	Blank Re (%)
Annobon A3							
Olivine 1	0.1344 ± 0.0011	0.1344	338	23.98	44.1	1.1	3.6
Olivine 2	0.1326 ± 0.0014	0.1325	273	39.61	33.6	0.7	4.8
Inclusion-rich olivine	0.1271 ± 0.0004	0.1271	1925	2654	3.53	0.1	4.5
Cpx 1	0.1338 ± 0.0005	0.1338	413	325.2	6.19	0.2	6.2
WR1	0.1280 ± 0.0003	0.1280	407	70.72	27.7	0.1	1.1
WR2	0.1283 ± 0.0002	0.1283	421	68.64	29.8	0.2	0.8
Annobon A7							
Olivine 1	0.1377 ± 0.0010	0.1376	132	37.35	26.7	0.4	5.5
Olivine 2	0.1359 ± 0.0012	0.1358	193	45.82	20.6	0.9	9.5
Inclusion-rich olivine 1	0.1295 ± 0.0004	0.1295	1756	1450	5.90	0.1	3.9
Inclusion-rich olivine 2	0.1309 ± 0.0006	0.1309	1996	958	10.15	0.2	3.9
WR1	0.1315 ± 0.0005	0.1315	205	91.53	10.8	0.1	2.2
WR2	0.1321 ± 0.0004	0.1321	212	93.80	11.0	0.2	1.7

[a] Age corrected.

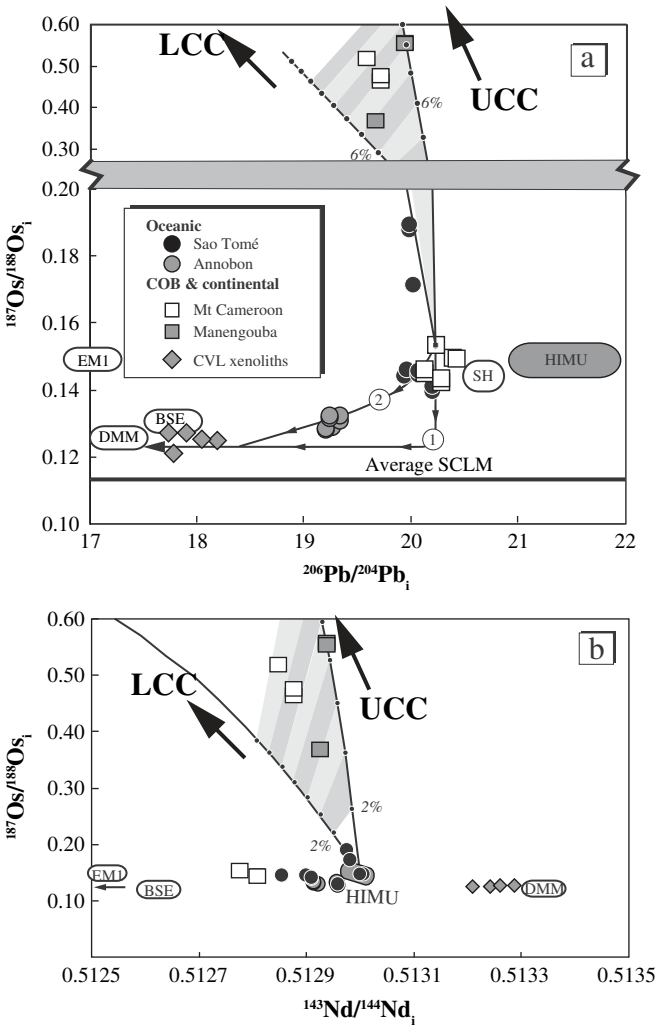

Fig. 7. $^{187}Os/^{188}Os$ versus (a) $^{206}Pb/^{204}Pb$ and (b) $^{143}Nd/^{144}Nd$ diagrams for CVL basalts. Pb and Nd isotope data are from Barfod (1999) and Lee et al. (1996). Approximate locations of the mantle components HIMU and DMM EM1, and the compositions representing the BSE are shown for reference. The average $^{187}Os/^{188}Os$ ratio for sub-continental lithospheric mantle is from Shirey and Walker (1998). Ultramafic xenoliths beneath continental part of the CVL are also shown. The Y-axis in the Os–Pb chart was truncated between 0.2 and 0.3 and the scale was changed between 0.3 and 0.6. The increments in the curves are 2%. The grey shaded area indicates the possible compositions for crustally contaminated lavas. The most radiogenic samples from the continental sector can be explained by assimilation of 8 to 16% of continental crust. Assuming for the uncontaminated starting point [Os] = 10 ppt, $^{187}Os/^{188}Os$ = 0.156, $^{206}Pb/^{204}Pb$ = 20.24, [Pb] = 2 ppm; for upper continental crust (UCC) [Os] = 50 ppt, $^{187}Os/^{188}Os$ = 1.4, $^{206}Pb/^{204}Pb$ = 19.3, [Pb] = 8 ppm; and for lower continental crust (LCC) [Os] = 50 ppt, $^{187}Os/^{188}Os$ = 0.8 (Saal et al., 1998), $^{206}Pb/^{204}Pb$ = 17.5, [Pb] = 8 ppm. Curves (1) and (2) describe the possible mixing trajectories between HIMU and DMM. (1) Assimilation of mantle xenocrysts and (2) mixing of lavas derived from DMM and HIMU sources. Modelling parameters are as follows: for (1) DMM mantle [Os] = 3 ppb, $^{187}Os/^{188}Os$ = 0.125, $^{206}Pb/^{204}Pb$ = 18.5, [Pb] = 0.15 ppm and for (2) DMM melt [Os] = 8 ppt, $^{187}Os/^{188}Os$ = 0.127, $^{206}Pb/^{204}Pb$ = 18.5, [Pb] = 0.45 ppm. For Os–Nd modelling the starting point was chosen to be the closest to HIMU endmember, $^{143}Nd/^{144}Nd$ = 0.513, [Nd] = 40 ppm, $^{187}Os/^{188}Os$ = 0.15, [Os] = 10 ppt; for UCC $^{143}Nd/^{144}Nd$ = 0.512, [Nd] = 27 ppm (Rudnick and Fountain, 1995), $^{187}Os/^{188}Os$ = 1.4, [Os] = 50 ppt; and for LCC $^{143}Nd/^{144}Nd$ = 0.512, [Nd] = 50 ppm (Kwékam et al., 2013), $^{187}Os/^{188}Os$ = 0.8, [Os] = 30 ppt (Saal et al., 1998). Increments in the curves are 2%.

upper continental crusts. The average osmium isotope composition for the upper crust has been estimated to be ~1.26 (Esser and Turekian, 1993) or more recently ~1.05 (Peucker-Ehrenbrink and Jahn, 2001) although estimates for the lower crust range from 0.4 to 0.8 (Saal et al., 1998). The eruptive centres at Mt. Cameroon and Manengouba lie mainly on gneissic and granitic rocks of the Pan-African basement complex, which range in age from 0.6 to 2.1 Ga (Kwékam et al., 2013). This crystalline basement forms part of a mobile belt between the West Africa and Congo Craton, however, there is no published Os isotope data available for silicic crustal material from Pan-African basement. Nevertheless, one can estimate the expected present day $^{187}Os/^{188}Os$ by using the range of $^{187}Re/^{188}Os$ of 10 to 100 reported so far for crustal rocks (e.g. Esser and Turekian, 1993; Peucker-Ehrenbrink and Jahn, 2001; Saal et al., 1998). If crustal ages of 0.6–2.1 Ga and average $^{187}Re/^{188}Os$ of 34.5 (Peucker-Ehrenbrink and Jahn, 2001) are assumed for CVL upper continental crust, this yields a present day $^{187}Os/^{188}Os$ of between 0.4 and 1.4. Taking these values for the upper and lower continental crusts and that for the HIMU lavas, a mixing scenario is illustrated in Figs. 6 and 7a. In Pb–Os isotope space the continental lavas from the CVL with $^{206}Pb/^{204}Pb < 19.94$ fall within the field of crustal contamination (Fig. 7a). Such a contamination process would also account for the highest SiO_2 observed for these samples (Fig. 6) as the continental crust in general and granitic basement under continental CVL in particular, are characterised by high SiO_2 (i.e. 64–77 wt.%; Marzoli et al., 2000). The results of mixing calculations are consistent in both diagrams (Figs. 6 and 7a) and amounts between of 8 and 16% continental assimilation are required to explain the observed shift in $^{187}Os/^{188}Os$ ratios and the SiO_2 contents, where mixing trajectories indicate that both upper and lower continental crusts may have been involved. Therefore, such proportions of crustal assimilation do not appear to have significantly modified the Pb or Nd isotopes of basalts from the continental sector.

5.2. Nature of the Os-unradiogenic component involved in oceanic CVL

The range of $^{187}Os/^{188}Os$ isotope compositions observed in the oceanic lavas of the CVL is relatively smaller (from 0.128 to 0.19) by comparison to that seen in the continental. Lavas from Annobon, Sao Tomé and Principe possess distinctive Os isotope and elemental compositions (Fig. 5). The most radiogenic samples of the oceanic lavas are those with low contents of Os (<7 ppt). These are all from the island of Sao Tome and lie close to the same mixing trends that might explain the contaminated continental basalts for Os and Pb isotopes (Fig. 7a). The presence of granitic xenoliths up to 10 cm in diameter in a lava flow in the western part of the Sao Tomé island suggests that granitic basement rocks could be the source of such minor radiogenic additions (<2% assimilation, see Fig. 7a). However, the presence of old basaltic crust with radiogenic $^{187}Os/^{188}Os$, resulting from ^{187}Re decay since crystallisation, could also affect the Os isotopic ratios of OIB erupted on old oceanic lithosphere such as that underlying CVL (~130 Ma). Such a contamination process, albeit at a less significant level, has been proposed by Marcantonio et al. (1995) and Reisberg et al. (1993) for radiogenic samples from St. Helena and La Palma, respectively. However, these samples apart, most of the Sao Tomé lavas still exhibit the same characteristics that are close to HIMU end-member (Fig. 7).

The important result from the oceanic lavas is the nearly constant and relatively unradiogenic Os and Pb isotope ratios found in Annobon. The unradiogenic Os isotope compositions of the Annobon lavas require the existence of a mantle component characterised by an unradiogenic $^{187}Os/^{188}Os$ isotope composition (<0.128). The observation in sample A3 of resorbed, strained crystals and polycrystalline fragments of olivine along with the presence of harzburgite xenoliths in the flow clearly indicates the presence of xenocrystic material probably from the suboceanic mantle (Fig. S1). This is supported by the high Fo content (>90%) in many olivine crystals (Fig. S2). Such origin is also supported by the unradiogenic Os isotope ratios and the high Os concentrations found in the inclusion-rich olivines as they plot close to mantle xenoliths from CVL (Fig. 5). The difference between the $^{187}Os/^{188}Os$ signature of the whole rock and inclusion-rich olivine is 0.7% for A3 and less than 1.5% for A7. However, optically pure olivine is up to 5% more radiogenic than the whole rock. If the optically pure olivine is largely magmatic

(rather than of mantle origin) then the $^{187}Os/^{188}Os$ signatures of such olivine are likely to be closer to the primary magmatic Os isotope ratios, because unlike the whole rock they are not affected by any mantle xenocrystic contribution.

The peridotite dominated part of the MORB mantle as defined by unaltered abyssal peridotites (Harvey et al., 2006; Snow and Reisberg, 1995) and the most unradiogenic MORB themselves (Gannoun et al., 2007) have low $^{187}Os/^{188}Os$ ratios ranging from 0.118 to 0.130. Therefore, at first sight the covariations between Os and Pb appear consistent with mixing of two mantle components, one with unradiogenic Os and Pb akin to DMM and another with radiogenic Os and Pb, i.e. the HIMU mantle. However, the relationship between $^{187}Os/^{188}Os$ isotope and Os concentration is unexpected, because melts that originate from the DMM usually possess relatively low Os concentrations (Gannoun et al., 2007) in contrast to the high concentrations observed here. Rather it seems more likely that the lavas possessing unradiogenic Os isotope compositions have themselves been contaminated by the physical entrainment of fragments of mantle material (i.e. xenoliths and xenocrysts) that possess very high Os concentrations.

However, while such physical contamination can readily explain the shift of Os isotopes, the mixing calculations suggest that this process cannot account alone for the shift of the Pb isotope compositions of the lavas towards the observed values. This is because the average Pb concentration of HIMU lavas is ~2 ppm which is some 10–15 times higher than that of mantle rocks (0.1–0.2 ppm), whereas the Os concentration in HIMU lavas of $\sim 10^{-2}$ ppb is some 3 orders of magnitude less than the average value for abyssal peridotites. The principal difference in the behaviour of Os and Pb is that 90% of the Os is hosted in sulphide and this dominates the signature of the whole-rock (Alard et al., 2002; Burton et al., 1999; Harvey et al., 2010). Whereas, only <10% of the Pb is hosted in the sulphide and the whole rock has a composition that is only slightly displaced from that of silicates (Burton et al., 2012).

One consequence of the contrasting distribution of both elements in HIMU lavas and oceanic mantle is that the mixing will be dominated by Os at the values shown in Fig. 7a and produces hyperbolic mixing line that exhibits a substantial variation in $^{187}Os/^{188}Os$ ratios (0.156 to 0.128) with little accompanying variation of $^{206}Pb/^{204}Pb$. The addition of 2–3% of mantle material can explain the elevated Os concentrations and the unradiogenic and narrow range of $^{187}Os/^{188}Os$ ratios observed in Annobon lavas (0.128–0.137). However, such a small addition of mantle material is not consistent with the low $^{206}Pb/^{204}Pb$ observed in Annobon lavas. It is concluded that while contamination by the physical entrainment of fragments of mantle material can account for the unradiogenic Os isotope compositions of some, it is not capable alone of producing the observed variations in Pb isotope compositions. Rather the observed shift for Pb isotopes is the result of mixing of lavas derived from DMM and HIMU sources. Hence the most plausible scenario to produce the Pb–Os geochemical characteristics of Annobon samples should include both processes that acted jointly.

These data highlight the challenge often faced in the interpretation of Os isotope data in basalts, in that Os poor basaltic magmas are highly sensitive to both physical and chemical contaminations, co-variations with other elements or isotopes cannot be assumed to be related to the same process, particularly when considered in isolation. In the present study any potential primary source variations in Os have been masked by the effects of physical contamination of the basalts.

5.3. Implications for the origin of the Cameroon volcanic line

Several models have been proposed for the formation of the CVL, generally they can be grouped into two categories, plume and non-plume models. Before considering the different petrogenetic models proposed for the origin of CVL, the major geochemical observations are summarised here.

If the data showing values beyond those encountered in OIB due to contamination by the continental crust are ignored, the range of $^{187}Os/^{188}Os$ and $^{206}Pb/^{204}Pb$ ratios reported in this study and elsewhere (Halliday et al., 1988; Lee et al., 1994) points to the involvement of two main mantle end-member reservoirs, depleted MORB upper mantle (DMM) and the so called high-μ mantle (HIMU). There is no evidence for the involvement of EM1 end-member based on isotope data distribution in Pb–Os–Nd space. Such involvement was reported by Lee et al. (1994) on the basis of Pb–Sr–Nd isotope variations for Annobon lavas. However, only Pb isotopes vary within oceanic islands of the CVL. Furthermore unradiogenic and more restricted Os and Pb isotope ratios in Annobon lavas do not require such an enriched component. It is widely considered that radiogenic Pb and Os isotope ratios seen in HIMU basalts reflect the presence of basaltic material that has been recycled back into the mantle at subduction zones (Hofmann, 1997). Recycled oceanic crust likely possesses elevated U/Pb and Re/Os ratios relative to the bulk silicate Earth, and if isolated for a long period of time (e.g. 0.5–2 Ga; Becker, 2000; Dale et al., 2007), will evolve to radiogenic Pb and Os isotope compositions. Therefore, the HIMU component is likely to originate from boundary layers in the mantle, where this long term isolation can occur (Allègre and Turcotte, 1985; Davies and Richards, 1992; Loper, 1991), which may be located either above the 660 km seismic discontinuity or above the core–mantle boundary at 2900 km.

As reported earlier, CVL comprises 12 major volcanic centres, the products of which range in age from 30 Ma to the present. In addition there are 17 plutonic complexes in the continental sector, which range in age from 65 to 30 Ma (Cantagrel et al., 1978; Fitton and Dunlop, 1985; Lasserre, 1978). There has been no systematic change in the focus of magmatism during this entire period (Fitton and Dunlop, 1985). Because the African plate has moved during the past 65 Ma, the absence of any migration or age progression of the volcanic centres is at odds with conventional hotspot models (Fitton and Dunlop, 1985; Halliday et al., 1988, 1990). Such observations rule out the hypothesis of single stationary plume anchored in the deep mantle beneath the CVL.

Spatial and temporal variations in Pb isotope ratios observed in the oceanic sector of the CVL led some authors to suggest a model of gradual incorporation of a HIMU component with time as older lavas at a given locality tend to have less radiogenic Pb and become more radiogenic for recent basalts (e.g. <10 Ma; Halliday et al., 1990; Lee et al., 1994). All investigated samples in this study, except one, were young so it is not possible to confirm the existence of any temporal variations in the osmium isotope composition. For instance samples P119 and P102 from Principe island (which are 20.6 and 5.9 Ma old, respectively) yield similar $^{187}Os/^{188}Os$ compositions of 0.133 and 0.128, respectively. At least with these two samples no noticeable temporal variation of $^{187}Os/^{188}Os$ is detected. However more data is still needed to draw robust statement on temporal evolution for Os isotopes. To illustrate the magnitude of the geographical control on the distribution of $^{187}Os/^{188}Os$ and $^{206}Pb/^{204}Pb$, the ranges of uncontaminated samples against the normalised distance for each locality from Annobon are shown in Fig. 8. This figure shows that for relatively young lavas (<10 Ma) there is no systematic decrease of $^{206}Pb/^{204}Pb$ and $^{187}Os/^{188}Os$ from the COB towards the oceanic end of the CVL. The space variation for both isotope ratios observed in the oceanic sector of the CVL does not support the model of gradual incorporation of HIMU component (Lee et al., 1994). Principe which is closer to the COB should be more radiogenic than S. Tomé and Annobon which is not the case. While the source in the COB seems to be enriched, the Os–Pb systematics in Annobon Island are similar to that observed in many Atlantic MORBs (Gannoun et al., 2007; Hofmann, 1997). This is intriguing because Annobon lavas share in the same time trace element pattern similar to the rest of the CVL (Lee et al., 1994). Principe, S. Tomé and Annobon are unlikely to originate from the same mantle source since each island seems to record different positions in Os–Pb isotope ratio space. It seems that each island is fed by individual and small scale thermal upwelling. Such configuration is in agreement to what was suggested by Burke (2001) who proposed that a change in

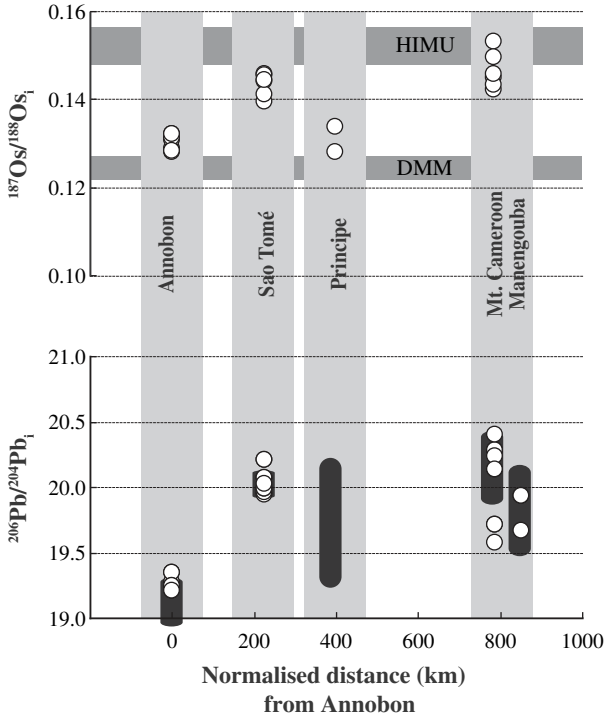

Fig. 8. Comparison of $^{187}Os/^{188}Os$ and $^{206}Pb/^{204}Pb$ ratios along the oceanic sector of the CVL. Plotted isotope ratio data for Os are from this study and the corresponding Pb isotope data are from Barfod (1999). Samples with highly radiogenic Os are excluded from the diagrams (crustal contamination). The black boxes represent data compilation from literature. Lead data are from Halliday et al. (1988, 1990) and Lee et al. (1994). Volcanoes at the COB show the highest $^{187}Os/^{188}Os$ and $^{206}Pb/^{204}Pb$. Annobon which is at the end of the oceanic sector of the CVL possesses MORB like signature for Os and Pb isotope ratios. More Os analyses are clearly needed for Principe to constrain the overall variability in this island.

plate motion around 30 Ma may have generated new upper mantle small-scale convection cells (~100 km diameter), and this slowdown could explain the increase of volcanism intensity around 30 Ma as result of increasing the strength of the convective flow regime. However, if such a hypothesis can explain the geochemical data in the oceanic sector it does not explain the much older plutonic activity in the continental sector (30–65 Ma) nor indeed the mechanism of melting.

Using their new evidence on seismic velocity in the upper mantle beneath western Africa, Reusch et al. (2010) discussed the implications of their tomographic images for geodynamic models that address the origin of the CVL. Both P and S waves show that the thermal anomaly continues along the CVL onshore and offshore and yield a nearly uniform transition zone thickness at depths of 410 and 660 km. This hot mantle is probably behind the observed negative gravity anomaly beneath CVL (Djomani et al., 1997). The near vertical sides of the anomaly and its extent at depth cannot be easily reconciled with the models of the origin of the CVL that invoke plumes (Burke, 2001; Ebinger and Sleep, 1998; Griffths and Campbell, 1990; Morgan, 1983) or decompression melting under reactivated shear zones (Fairhead and Binks, 1991). However it is consistent with a model invoking edge-flow convection driven by lateral variations of lithospheric thickness along the northern boundary of the Congo Craton lithosphere (King, 2007; King and Ritsema, 2000) especially for the continental volcanism. To explain the linear nature of the oceanic part, Reusch et al. (2010) suggest the upwelling of warm material in the convective eddy being channelled along the presumed location of the Cameroon Fracture Zone (Fig. 1). Upwelling could also cause the reactivation of preexisting Pan-African lithospheric fractures. However as edge-driven convection is a 'weak flow', it is probably only relevant after the African plate slowed down significantly (i.e. <30 Ma). Therefore since the oceanic lithosphere was developed at that time, edge-driven convection circumscribing the Congo Craton alone can explain the current distribution of volcanic centres, without calling on a special fracture-zone channelling mechanism, especially since the fracture zone is unlikely to affect the mantle at 300+ km depth. This model can explain the progressive feeding of volcanism starting at Principe and to the south-western islands of Sao Tomé and Annobon. It can also explain the delayed start of magmatic activity until 65 Ma because the convective eddy was not fully established.

6. Concluding remarks

Young alkali basalts (<10 Ma) from the Cameroon volcanic line indicate a clear geographical control on the variability of Os isotopes, showing parallels with Pb isotopes. As for Pb, the Os isotope composition of "uncontaminated" lavas is found to be present at the continent–ocean boundary zone at Mt Cameroon, where the HIMU signature attributed to these lavas shows the Os isotopic signature of ~0.15–0.16, consistent with the Os composition attributed to HIMU elsewhere (e.g. Hauri and Hart, 1993; Marcantonio et al., 1995; Reisberg et al., 1993; Schiano et al., 2001). Many other nearby samples from the continental sector yield unexpectedly radiogenic $^{187}Os/^{188}Os$ compositions between 0.36 and 0.56, outside the range of other ocean island basalts. Lavas at these localities have most probably interacted with continental crust leading to increasingly radiogenic $^{187}Os/^{188}Os$, higher SiO_2 and a shift to less radiogenic $^{206}Pb/^{204}Pb$ ratios. Simple modelling suggests that between 8 and 16% of crustal contamination has occurred and that both upper and lower continental crust could have been involved. Such a process appears to have not significantly modified the Nd isotopic compositions. Ultramafic xenoliths from the SCLM beneath continental sector of CVL yield without exception unradiogenic, sub-chondritic, $^{187}Os/^{188}Os$ compositions ruling out the involvement of sub-continental lithospheric mantle for the radiogenic Os isotope ratios observed in the continental CVL lavas.

In contrast, for the oceanic sector the systematic shift in lead isotope composition to unradiogenic values from the COB ocean-wards is positively correlated with decreases in $^{187}Os/^{188}Os$ (from 0.140 to 0.128). This co-variation might be attributed to the mixing of plume material (HIMU) with the ambient upper mantle (DMM) leading to the decrease of $^{206}Pb/^{204}Pb$. However, the Os isotope and Os and Ni elemental variations are more readily explained by the presence of mantle material (xenoliths and xenocrysts) that contaminate the mantle derived melts. This is consistent with the Re–Os isotope data for minerals separated from the oceanic basalts. In particular, these data indicate that inclusion-rich olivine possesses an unradiogenic Os isotope composition consistent with a mantle origin. Overall, these results indicate that for osmium isotope system mantle derived basalts, both OIB and MORB, are highly susceptible to contamination, and covariations with other isotopes and/or elements must be interpreted with caution.

Acknowledgements

This work was partially supported by the Natural Environment Research Council (under contract NER/A/S/2001/00538). This research was financed by the French Government Laboratory of Excellence initiative no. ANR-10-LABX-0006, the Région Auvergne and the European Regional Development Fund. This is Laboratory of Excellence ClerVolc contribution number 129. We are also grateful for the constructive reviews of A. Marzoli and one anonymous reviewer which led to the improvement of the manuscript. We thank Sun-Lin Chung for editorial handling.

Appendix A. Supplementary data

Supplementary data to this article can be found online at http://dx.doi.org/10.1016/j.lithos.2015.02.017.

References

Aka, F.T., Nagao, K., Kusakabe, M., Sumino, H., Tanyileke, G., Ateba, B., Hell, J., 2004. Symmetrical helium isotope distribution on the Cameroon volcanic line, West Africa. Chemical Geology 203, 205–223.

Alard, O., Griffin, W.L., Pearson, N.J., Lorand, J.-P., O'Reilly, S.Y., 2002. New insights into the Re–Os systematics of subcontinental lithospheric mantle from in-situ analysis of sulfides. Earth and Planetary Science Letters 203, 651–663.

Allègre, C.J., Luck, J.-M., 1980. Osmium isotopes as petrogenetic and geological tracers. Earth and Planetary Science Letters 48, 148–154.

Allègre, C.J., Turcotte, D.L., 1985. Geodynamic mixing in the mesosphere boundary layer and the origin of oceanic islands. Journal of Geophysical Research 12, 207–210.

Alves, S., Schiano, P., Capmas, F., Allègre, C.J., 2002. Osmium isotope binary mixing arrays in arc volcanism. Earth and Planetary Science Letters 198, 355–369.

Barfod, D.N., 1999. Noble Gas Geochemistry of the Cameroon Line Volcanic Chain. (Ph. D. thesis). Michigan Univ.

Becker, H., 2000. Re–Os fractionation in eclogites and blueschists and the implications for recycling of oceanic crust into the mantle. Earth and Planetary Science Letters 177, 287–300.

Becker, H., Horan, M.F., Walker, R.J., Gao, S., Lorand, J.-P., Rudnick, R.L., 2006. Highly siderophile element composition of the Earth's primitive upper mantle: constraints from new data on peridotite massifs and xenoliths. Geochimica et Cosmochimica Acta 70, 4528–4550.

Bennett, V.C., Esat, T.M., Norman, M.D., 1996. Two mantle-plume components in Hawaiian picrites inferred from correlated Os–Pb isotopes. Nature 381, 221–224.

Birck, J.L., Roy-Barman, M., Capmas, F., 1997. Re–Os isotopic measurements at femtomole level in natural samples, Geostandards. Newsletter 20, 19–27.

Borg, L.E., Brandon, A.D., Clynne, M.A., Walker, R.J., 2000. Re–Os isotopic systematics of primitive lavas from the Lassen region of the Cascade arc, California. Earth and Planetary Science Letters 177, 301–317.

Burke, K., 2001. Origin of the Cameroon line of volcano-capped swells. Journal of Geology 109, 349–362.

Burton, K.W., Schiano, P., Birck, J.L., Allègre, C.J., 1999. Osmium isotope disequilibrium between mantle minerals in a spinel–lherzolite. Earth and Planetary Science Letters 172, 311–322.

Burton, K.W., Schiano, P., Birck, J.L., Allègre, C.J., Rehkämper, M., Halliday, A.N., Dawson, J.B., 2000. The distribution and behaviour of rhenium and osmium amongst mantle minerals and the age of the lithospheric mantle beneath Tanzania. Earth and Planetary Science Letters 183, 93–106.

Burton, K.W., Gannoun, A., Birck, J.L., Allègre, C.J., Schiano, P., Clocchiatti, R., Alard, O., 2002. The compatibility of rhenium and osmium in natural olivine and their behaviour during mantle melting and basalt genesis. Earth and Planetary Science Letters 198, 63–76.

Burton, K.W., Cenki-Tok, B., Mokadem, F., Harvey, J., Gannoun, A., Alard, O., Parkinson, I.J., 2012. Unradiogenic lead in Earth's upper mantle. Nature Geoscience 5, 570–573.

Cantagrel, J.-M., Jamond, C., Lasserre, M., 1978. Le magmatisme alkalin de la ligne du Cameroun au Tertiaire inferieur: donnees géochronologiques K/Ar. Compte Rendu. Sommaire des Séances. Société Géologique de France 6, 300–303.

Chase, C.G., 1981. Oceanic island Pb: two-stage histories and mantle evolution. Earth and Planetary Science Letters 52, 277–284.

Chauvel, C., Hofmann, A.W., Vidal, P., 1992. HIMU-EM: the French Polynesian connection. Earth and Planetary Science Letters 110, 99–119.

Chesley, J., Ruiz, J., Righter, K., Ferrari, L., Gomez-Tuena, A., 2002. Source contamination versus assimilation: an example from the Trans-Mexican volcanic arc. Earth and Planetary Science Letters 195, 211–221.

Class, C., Goldstein, S.L., Shirey, S.B., 2009. Osmium isotopes in Grande Comore lavas: a new extreme among a spectrum of EM-type mantle endmembers. Earth and Planetary Science Letters 284, 219–227.

Cohen, A.S., Waters, F.G., 1996. Separation of osmium from geological materials by solvent extraction for analysis by thermal ionisation mass spectrometry. Analytica Chimica Acta 332, 269–275.

Conway, F.M., Ferrill, D.A., Hall, C.M., Morris, A.P., Stamatakos, J.A., Connor, C.B., Halliday, A.N., Condit, C., 1997. Timing of basaltic volcanism along the Mesa Butte Fault in the San Francisco volcanic field, Arizona, from $^{40}Ar/^{39}Ar$ dates: implications for longevity of cinder cone alignments. Journal of Geophysical Research 102, 815–824.

Dale, C.W., Gannoun, A., Burton, K.W., Argles, T.W., Parkinson, I.J., 2007. Rhenium–osmium isotope and elemental behaviour during subduction of oceanic crust and the implications for mantle recycling. Earth and Planetary Science Letters 253, 211–225.

Davies, G.F., Richards, M.A., 1992. Mantle convection. Journal of Geology 100, 151–206.

DePaolo, D.J., 1981. Trace element and isotopic effects of combined wallrock assimilation and fractional crystallization. Earth and Planetary Science Letters 53, 189–202.

Djomani, Y.H.P., Diament, M., Wilson, M., 1997. Lithospheric structure across the Adamawa plateau (Cameroon) from gravity studies. Tectonophysics 273, 317–327.

Ebinger, C.J., Sleep, N.H., 1998. Cenozoic magmatism throughout east Africa resulting from impact of a single plume. Nature 395, 788–791.

Eisele, J., Sharma, M., Galer, S.J.G., Blichert-Toft, J., Devey, D.W., Hofmann, A.W., 2002. The role of sediment recycling in EM-1 inferred from Os, Pb, Hf, Nd, Sr isotope and trace element systematics of the Pitcairn hotspot. Earth and Planetary Science Letters 196, 197–212.

Esser, B.K., Turekian, K.K., 1993. The osmium isotopic composition of the continental crust. Geochimica et Cosmochimica Acta 57, 3093–3104.

Fairhead, J.D., Binks, R.M., 1991. Differential opening of the Central and South Atlantic oceans and the opening of the West African rift system. Tectonophysics 187, 191–203.

Fischer-Gödde, M., Becker, H., Wombacher, F., 2010. Rhodium, gold and other highly siderophile element abundances in chondritic meteorites. Geochimica et Cosmochimica Acta 74, 356–379.

Fitton, J.G., 1987. The Cameroun line, West Africa: a comparison between oceanic and continental alkaline volcanism. Geological Society, London, Special Publications 30, 273–291.

Fitton, J.G., Dunlop, H.M., 1985. The Cameroon line, West Africa, and its bearing on the origin of oceanic and continental alkali basalt. Earth and Planetary Science Letters 72, 23–38.

Gannoun, A., Burton, K.W., Thomas, L.E., Parkinson, I.J., Van-Calsteren, P.W., Schiano, P., 2004. Osmium isotope heterogeneity in the constituent phases of mid-ocean ridge basalts. Science 303, 70–72.

Gannoun, A., Burton, K.W., Parkinson, I.J., Alard, O., Schiano, P., Thomas, L.E., 2007. The scale and origin of the osmium isotope variations in mid-ocean ridge basalts. Earth and Planetary Science Letters 259, 541–556.

Gleißner, P., Drüppel, K., Becker, H., 2012. Osmium isotopes and highly siderophile element fractionation in the massif-type anorthosites of the Mesoproterozoic Kunene Intrusive Complex, NW Namibia. Chemical Geology 302–303, 33–47.

Griffths, R.W., Campbell, I.H., 1990. Stirring and structure in mantle starting plumes. Earth and Planetary Science Letters 99, 66–78.

Halliday, A.N., Dickin, A.P., Fallick, A.E., Fitton, J.G., 1988. Mantle dynamics: a Nd, Sr, Pb and O isotopic study of the Cameroon line volcanic chain. Journal of Petrology 29, 181–211.

Halliday, A.N., Davidson, J.P., Holden, P., De Wolf, C., Lee, D.-C., Fitton, J.G., 1990. Trace-element fractionation in plumes and the origin of HIMU mantle beneath the Cameroon line. Nature 347, 523–528.

Hart, S.R., 1988. Heterogeneous mantle domains: signatures, genesis and mixing chronologies. Earth and Planetary Science Letters 90, 273–296.

Hart, W.K., Carlson, R.W., Shirey, S.B., 1997. Radiogenic Os in primitive basalts from the northwestern U.S.A.: implications for petrogenesis. Earth and Planetary Science Letters 150, 103–116.

Harvey, J., Gannoun, A., Burton, K.W., Rogers, N.W., Alard, O., Parkinson, I.J., 2006. Ancient melt extraction from the oceanic upper mantle revealed by Re–Os isotopes in abyssal peridotites from the Mid-Atlantic ridge. Earth and Planetary Science Letters 244, 606–621.

Harvey, J., Gannoun, A., Burton, K.W., Rogers, N.W., Schiano, P., Alard, O., 2010. Unravelling the effects of melt depletion and secondary infiltration on mantle Re–Os isotopes beneath the French Massif Central. Geochimica et Cosmochimica Acta 74, 293–320.

Hauri, E.H., Hart, S.R., 1993. Re-Os isotope systematics of HIMU and EMII oceanic island basalts from the south Pacific Ocean. Earth and Planetary Science Letters 114, 353–371.

Hauri, E.H., Lassiter, J.C., DePaolo, D.J., 1996. Os isotope systematics of drilled lavas from Mauna Loa, Hawaii. Journal of Geophysical Research 101, 11793–11806.

Hofmann, A.W., 1997. Mantle geochemistry: the message from oceanic volcanism. Nature 385, 219–229.

Hofmann, A.W., White, W.M., 1982. Mantle plumes from ancient oceanic crust. Earth and Planetary Science Letters 57, 421–436.

Jacquemin, H., Sheppard, S.M.F., Vidal, P., 1982. Isotopic geochemistry (O, Sr, Pb) of the Golda Zuelva and M'boutou anorogenic complexes, North Cameroon: mantle origin with evidence for crustal contamination. Earth and Planetary Science Letters 61, 97–111.

King, S.D., 2007. Hotspots and edge-driven convection. Geology 35, 223–226.

King, S.D., Ritsema, J., 2000. African hot spot volcanism: small-scale convection in the upper mantle beneath cratons. Science 290, 1137–1140.

Kwékam, M., Affaton, P., Bruguier, B., Liégeois, J.P., Hartmann, G., Njonfang, E., 2013. The Pan-African Kekem gabbro-norite (West-Cameroon), U–Pb zircon age, geochemistry and Sr–Nd isotopes: geodynamical implication for the evolution of the Central African fold belt. Journal of African Earth Sciences 84, 70–88.

Lasserre, M., 1978. Mise au point sur les granitoides dits “ultimes” du Cameroun: gisement, pétrographie et géochronologie. Bull. Bur. Rech. Geol. Min. Sect. IV 2, pp. 143–159.

Lassiter, J.C., Hauri, E.H., 1998. Osmium-isotope variations in Hawaiian lavas: evidence for recycled oceanic lithosphere in the Hawaiian plume. Earth and Planetary Science Letters 164, 483–496.

Lassiter, J.C., Luhr, J.F., 2001. Osmium abundance and isotope variations in mafic Mexican volcanic rocks: evidence for crustal contamination and constraints on the geochemical behavior of osmium during partial melting and fractional crystallization. Geochemistry, Geophysics, Geosystems 2, 1027. http://dx.doi.org/10.1029/2000GC000116.

Lee, D.-C., Halliday, A.N., Fitton, J.G., Poli, G., 1994. Isotopic variations with distance and time in the volcanic islands of the Cameroon line: evidence for a mantle plume origin. Earth and Planetary Science Letters 123, 119–138.

Lee, D.-C., Halliday, A.N., Davies, G.R., Essene, E.J., Fitton, J.G., Temdjim, R., 1996. Melt enrichment of shallow depleted mantle: a detailed petrological, trace element and isotopic study of mantle-derived xenoliths and megacrysts from the Cameroon line. Journal of Petrology 37, 415–441.

Loper, D., 1991. Mantle plumes. Tectonophysics 187, 373–384.

Marcantonio, F.A., Zindler, A., Staudigel, H., Schmincke, H., 1995. Os isotope systematics of La Palma, Canary Islands: evidence for recycled crust in the mantle source of HIMU ocean islands. Earth and Planetary Science Letters 133, 397–410.

Marzoli, A., Renne, P.R., Piccirillo, E.M., Francesca, C., Bellieni, G., Melfi, A.J., Nyobe, J.B., N'ni, J., 1999. Silicic magmas from the continental Cameroon volcanic line (Oku, Bambouto and Ngaoundere): $^{40}Ar–^{39}Ar$ dates, petrology, Sr–Nd–O isotopes and their petrogenetic significance. Contributions to Mineralogy and Petrology 135, 133–150.

Marzoli, A., Piccirillo, E.M., Renne, P.R., Bellieni, G., Iacumin, M., Nyobe, J.B., Tongwa, A.T., 2000. The Cameroon volcanic line revisited: petrogenesis of continental basaltic

magma from lithospheric and asthenospheric mantle sources. Journal of Petrology 41, 87–109.
McDonough, W.F., Sun, S.-S., 1995. The composition of the Earth. Chemical Geology 120, 223–253.
Meisel, T., Walker, R.J., Morgan, J.W., 1996. The osmium isotopic composition of the Earth's upper mantle. Nature 383, 517–520.
Meisel, T., Walker, R.J., Irving, A.J., Lorand, J.-P., 2001. Osmium isotopic composition of mantle xenoliths: a global perspective. Geochimica et Cosmochimica Acta 65, 1311–1323.
Meisel, T., Reisberg, L., Moser, J., Carignan, J., Melcher, F., Brugmann, G., 2003. Re–Os systematics of UB–N, a serpentinized peridotite reference material. Chemical Geology 201, 161–179.
Morgan, W.J., 1983. Hotspot tracks and the early rifting of the Atlantic. Tectonophysics 94, 123–139.
Morgan, J.W., 1986. Ultramafic xenoliths: clues to Earths late accretionary history. Journal of Geophysical Research 91, 12375–12387.
Morin, D., Corriveau, L., 1996. Fragmentation processes and xenolith transport in Proterozoic minette dyke, Grenville Province, Quebec. Contributions to Mineralogy and Petrology 125, 319–331.
Nowell, G.M., Luguet, A., Pearson, D.G., Horstwood, M.A., 2008. Precise and accurate $^{186}Os/^{188}Os$ and $^{187}Os/^{188}Os$ measurements by multi-collector plasma ionisation mass spectrometry (MC-ICP-MS) part I: solution analyses. Chemical Geology 248, 363–393.
Parsons, I., Brown, W.L., Jacqcuemin, H., 1986. Mineral chemistry and crystallization conditions of the Mboutou layered gabbro-syenite–granite complex, North Cameroon. Journal of Petrology 27, 1305–1330.
Peucker-Ehrenbrink, B., Jahn, B.M., 2001. Rhenium–osmium isotope systematics and platinum group element concentrations: loess and the upper continental crust. Geochemistry, Geophysics, Geosystems 2 (10), 2200. http://dx.doi.org/10.1029/2001GC000172.
Rankenburg, K., Lassiter, J.C., Brey, G.P., 2005. The role of continental crust and lithospheric mantle in the genesis of Cameroon volcanic line lavas: constraints from isotopic variations in lavas and megacrysts from the Biu and Jos Plateaux. Journal of Petrology 46, 169–190.
Rehkämper, M., Halliday, A.N., Barfod, D., Fitton, J.G., Dawson, J.B., 1997. Platinum-group element abundance patterns in different mantle environments. Science 278, 1595–1598.
Reisberg, L., Lorand, J.P., 1995. longevity of the sub-continental mantle lithosphere from osmium isotope systematics in orogenic lherzolite massifs. Nature 376, 159–162.
Reisberg, L., Zindler, A., Marcantonio, F., White, W., Wyman, D., Weaver, B., 1993. Os isotope systematics in ocean island basalts. Earth and Planetary Science Letters 120, 149–167.
Reusch, A.M., Nyblade, A.A., Wiens, D.A., Shore, P.J., Ateba, B., Tabod, C.T., Nnange, J.M., 2010. Upper mantle structure beneath Cameroon from body wave tomography and the origin of the Cameroon volcanic line. Geochemistry, Geophysics, Geosystems 11, Q10W07. http://dx.doi.org/10.1029/2010GC003200.
Roy-Barman, M., Allègre, C.J., 1995. $^{187}Os/^{186}Os$ in oceanic island basalts: tracing oceanic crust recycling in the mantle. Earth and Planetary Science Letters 129, 145–161.
Rudnick, R.L., Fountain, D.M., 1995. Nature and composition of the continental crust: a lower crustal perspective. Reviews of Geophysics 33, 267–309.
Saal, A.E., Rudnick, R.L., Ravizza, G.E., Hart, S.R., 1998. Re–Os isotope evidence for the composition, formation and age of the lower continental crust. Nature 393, 58–61.
Scarfe, C.M., Brearly, M., 1987. Mantle xenoliths: melting and dissolution studies under volatile-free conditions. In: Nixon, P.H. (Ed.), Mantle Xenoliths. John Wiley and Sons, pp. 599–608.
Schiano, P., Birck, J.L., Allègre, C.J., 1997. Osmium–strontium–neodymium–lead isotopic covariations in mid-ocean ridge basalts glasses and the heterogeneity of the upper mantle. Earth and Planetary Science Letters 150, 363–379.
Schiano, P., Burton, K.W., Dupré, B., Birck, J.L., Guille, G., Allègre, C.J., 2001. Correlated Os–Pb–Nd–Sr isotopes in the Austral–Cook chain basalts: the nature of mantle components in plume sources. Earth and Planetary Science Letters 186, 527–537.
Schlüter, T., 2006. Geological Atlas of Africa: With Notes on Stratigraphy, Tectonics, Economic Geology, Geohazards and Geosites of Each Country. 1st ed. Springer, New York.
Shirey, S.B., Walker, R.J., 1998. The Re–Os isotope system in cosmochemistry and high-temperature geochemistry. Annual Review of Earth and Planetary Sciences 26, 423–500.
Sibuet, J.C., Mascle, J., 1978. Plate kinematic implications of Atlantic equatorial fracture zone trends. Journal of Geophysical Research 83, 3401–3421.
Skovgaard, A.C., Storey, M., Baker, J., Blusztajn, J., Hart, S.R., 2001. Osmium–oxygen isotopic evidence for a recycled and strongly depleted component in the Iceland mantle plume. Earth and Planetary Science Letters 194, 259–275.
Snow, J.E., Reisberg, L., 1995. Os isotopic systematics of the MORB mantle: results from altered abyssal peridotites. Earth and Planetary Science Letters 133, 411–421.
Suh, C.E., Sparks, R.S.J., Fitton, J.G., Ayonghe, S.N., Annen, C., Nana, R., Luckman, A., 2003. The 1999 and 2000 Eruptions of Mount Cameroon: eruption behaviour and petrochemistry of lava. Bulletin of Volcanology 65, 267–281.
Walker, R.J., Horan, M.F., Morgan, J.W., Becker, H., Grossman, J.N., Rubin, A.E., 2002. Comparative $^{187}Re–^{187}Os$ systematics of chondrites: implications regarding early solar system processes. Geochimica et Cosmochimica Acta 66, 4187–4201.
White, W.M., 1985. Sources of oceanic basalts: radiogenic isotope evidence. Geology 13, 115–118.
Widom, E., Hoernle, K.A., Shirey, S.B., Schminke, H.-U., 1999. Os isotope systematics in the Canary Islands and Madeira: lithospheric contamination and mantle plume signatures. Journal of Petrology 40, 279–296.
Woodhead, J., 1996. Extreme HIMU in an oceanic setting: the geochemistry of Mangaia Island (Polynesia), and temporal evolution of the Cook–Austral hotspot. Journal of Volcanology and Geothermal Research 72, 1–19.
Yokoyama, T., Aka, F.T., Kusakabe, M., Nakamura, E., 2007. Plume–lithosphere interaction beneath Mt. Cameroon volcano, West Africa: constraints from 238U–230Th–226Ra and Sr–Nd–Pb isotope systematics. Geochimica et Cosmochimica Acta 71, 1835–1854.
Zindler, A., Hart, S.R., 1986. Chemical geodynamics. Annual Review of Earth and Planetary Sciences 14, 493–571.